Mechanisms of Reinforcement Benefit from Geosynthetics Used as Subgrade Stabilization

E. Cuelho

Western Transportation Institute, Montana State University, USA (elic@montana.edu)

S. Perkins

Civil Engineering Department, Montana State University, USA (stevep@montana.edu)

ABSTRACT: Geogrids and geotextiles are routinely used to stabilize weak subgrade soils during road construction. Typical subgrade stabilization applications are temporary haul roads or unpaved low-volume roads, but can also include paved roads built on poorer foundation materials. Full-scale tests were constructed, trafficked and monitored (in two distinct phases) to compare the relative operational performance of geosynthetics used as subgrade stabilization, as well as determine which material properties are most related to performance. During the separate phases of this project, test sections were constructed using ten different geosynthetics (Phase I) and twelve different geosynthetics (Phase II), both consisting of geogrids and geotextiles. Multiple control test sections were also built to evaluate the effect that subgrade strength, base course thickness, and/or presence of the geosynthetic had on performance. Using longitudinal rut as the primary indicator of performance, it was determined through a linear regression analysis that the strength and stiffness of the junctions and tensile strength properties in the cross-machine direction correlated well with performance in this application, depending on the level of surface distress. Furthermore, instrumentation installed during the field experiment helped describe the behavior of the geosynthetics as rut developed under trafficking loads. Instrumentation consisted of displacement measurements using linear variable differential transformers (LVDTs) and strain measurements using bonded strain gages. Data from these instruments helped describe the method of reinforcement the geosynthetic provided as it transitioned from lateral confinement of the base layer to tensioned-membrane support, and how this transition related to rutting at the road surface.

Keywords: geosynthetics, stabilization, performance, junction stiffness

1 INTRODUCTION

Geogrids and geotextiles are routinely used for subgrade stabilization applications. This construction practice involves placing a geosynthetic on top of a weak subgrade to help stabilize the ground in order to construct the remaining gravel platform. The geosynthetic generally provides stabilization of the subgrade by increasing the load-carrying capacity of the system and maintaining separation between the soft subgrade and subbase materials. Subgrade stabilization allows a firm construction platform to be built with less aggregate and less construction time as compared to construction without the stabilization geosynthetic. Typical applications are temporary haul roads or unpaved low-volume roads. There is a general consensus concern-

ing the effectiveness of geosynthetics in this application; however, there is a lack of understanding and agreement on which geosynthetic material properties best relate to their performance. Those properties should be specified or used in design to ensure its beneficial use and to allow a broad range of products to be considered.

The main objective of this project was to determine material properties of geosynthetics most related to the in-field performance of geosynthetics used for subgrade stabilization, so that designers can objectively and confidently specify appropriate geosynthetics based on material properties and cost for a specific situation, while also allowing competition from different manufacturers. To accomplish this, test sections were constructed at a controlled test site to investigate the relative benefit to an unpaved road of various geosynthetics available on the market at the time. A subgrade soil was constructed in a weak state to provide equivalent conditions for each test section; likewise, the gravel surfacing along the entire test bed was uniformly constructed to be able to make direct comparisons between geosynthetic products. Longitudinal rut from traffic loading was the primary indicator of performance benefits of each geosynthetic. Material properties including wide-width tensile strength, cyclic tensile modulus, resilient interface shear stiffness, junction strength, and aperture stability modulus were used in a regression analysis to determine their relationship to performance in this application.

The objectives of this research were accomplished through a comprehensive program that included constructing, monitoring and analyzing full-scale field test sections as well as extensive laboratory tests on geosynthetics (Cuelho et al., 2014). Seventeen test sections were constructed, trafficked and monitored during summer 2012 to evaluate geosynthetics when used as subgrade stabilization. Design of this experiment was based on a previous phase (Phase I) completed in 2009 (Cuelho and Perkins, 2009) and centered on providing a uniform platform to evaluate the performance of multiple geosynthetics and other unpaved road design characteristics. The conditions in Phase I were more severe than in Phase II.

2 EXPERIMENTAL DESIGN

This research project was specifically planned to quantify differences in performance of various geosynthetic products under the same conditions (i.e., same subgrade strength and base course thickness). In addition, supplemental test sections were constructed to study the effect that variations in subgrade strength and base course thickness had on the performance. Specifically, three control sections (i.e., no geosynthetic) were constructed, each having different thickness of base course aggregate, and three test sections were built using the same integrally-formed geogrid (test sections IFG-1, IFG-2, and IFG-3), each having different subgrade strengths. The final arrangement of the test sections is shown in Figure 1, which includes the target subgrade strength and base thickness properties for construction (target California Bearing Ratio = 1.70 and target base thickness = 30.5 cm). Each test section was 4.9 m wide and 15 m long. The TRANSCEND research test facility managed by the Western Transportation Institute at Montana State University was used for this effort.

Twelve geosynthetic products (ten geogrids and two geotextiles) were used in this research project to evaluate their relative performance under the conditions presented herein. A summary of the basic material characteristics and strengths of these products is listed in Table 1. Five laboratory tests were used to characterize the geosynthetics used in this research, and include wide-width tensile strength (ASTM D 4595 and ASTM D 6637), cyclic tensile modulus (ASTM D 7556), resilient interface shear stiffness (ASTM D 7499), junction strength (ASTM D 7737), and aperture stability modulus (Kinney, 2000).

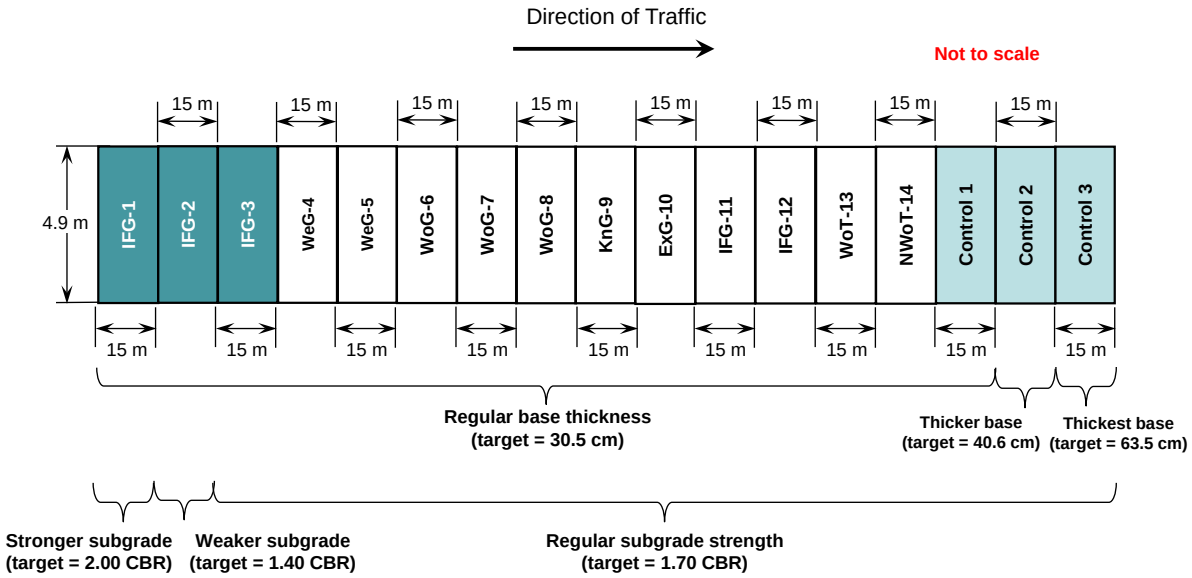

Figure 1: General layout of test sections with target construction parameters

Table 1: Summary of geosynthetic characteristics

Geosynthetic Test Section[a]	Polymer and Structure[b]	Mass per unit area (g/m^2)	Aperture Size (mm)	Strength @ 2% (kN/m)		Strength @ 5% (kN/m)		Ultimate Strength (kN/m)	
			MD x XMD	MD	XMD	MD	XMD	MD	XMD
IFG-1, IFG-2 and IFG-3	PP – integrally-formed, bi-axial geogrid	302	25 x 33	8.5	12.0	15.7	21.8	21.6	28.4
WeG-4	PP – vibratory-welded, bi-axial geogrid	200	33 x 33	14.1	13.8	26.4	26.7	30.4	39.6
WeG-5	PP – biaxial, welded geogrid	203	43 x 41	14.6	12.5	29.6	25.9	38.6	34.7
WoG-6	PMY – PVC-coated, woven, biaxial geogrid	322	25 x 25	5.8	9.0	10.0	13.5	29.8[f]	55.2[f]
WoG-7	PMY – PVC-coated, woven, biaxial geogrid	417	25 x 25	5.8	14.4	10.4	21.1	31.3[f]	84.9[f]
WoG-8	PMY – PVC-coated, woven, biaxial geogrid	309	25 x 25	9.4	10.8	20.1	18.7	38.4	47.0
KnG-9	PP – polymer-coated, knitted, biaxial geogrid	220	15 x 15	9.7	13.8	20.8	28.3	27.2	38.2
ExG-10[g]	PP – extruded, triple-layer, biaxial geogrid	329	43 x 51[c]	8.3	10.1	15.3	19.6	20.6	32.8
IFG-11	PP – integrally-formed, triaxial geogrid	180	41 x 41[d]	0.5[h]	4.7	2.6[h]	9.7	9.1[h]	12.3
IFG-12	PP – integrally-formed, triaxial geogrid	217	41 x 41[d]	1.0[h]	5.7	3.8[h]	10.9	11.0[h]	12.9
WoT-13	PPF – woven geotextile	417	40[e]	7.3	21.9	18.8	50.2	82.0	89.2
NWoT-14	PP – non-woven, needle-punched geotextile	271	80[e]	---	---	---	---	1.03[i]	1.13[i]

[a] Acronym meanings (related to manufacturing process): IFG = integrally-formed grid, WeG = welded grid, WoG = woven grid, KnG = knitted grid, ExG = extruded grid, WoT = woven textile, NWoT = non-woven textile; numbers represent position of test section
[b] PP = polypropylene, PMY = polyester multifilament yarn, PPF = polypropylene fiber
[c] for a single layer; apparent opening size is reduced when three layers are stacked on top of one another
[d] reported as "rib pitch" in manufacturer's specification sheet
[e] Apparent Opening Size (AOS) in U.S. Standard sieve size, ASTM D 4751
[f] WoG-6 and WoG-7 materials experienced some grip slippage at their ultimate strength values
[g] Tested as a composite, i.e., not separately (triple layer material)
[h] When the IFG-11 and IFG-12 geogrids are tested in the machine direction, tensile members are offset by 30 degrees from the direction of the applied load, resulting in large distortions of the material and lower and/or inaccurate strength values
[i] Grab tensile strength (ASTM D-4632) in kN
MD = machine direction; XMD = cross-machine direction

The soil used to construct the subgrade consisted of natural overburden material that classified as CL (sandy lean clay) according to the USCS classification system (ASTM D 2487). The base course material for this project consisted of crushed aggregates and classified as GP-GC (poorly graded gravel with clay with sand) according to the USCS classification system (ASTM D 2487). It contained 10 percent fines and 55 percent fractured faces. Laboratory strength tests run on the base course aggregate (ASTM D1883) resulted in a California Bearing Ratio (CBR) value greater than 100; however, in-field CBR tests indicated that the in-place CBR strength of the base varied between 25 and 75.

3 CONSTRUCTION OF FIELD EXPERIMENT

Construction of the test sections began with preparing and placing the subgrade, followed by installing the geosynthetics and instrumentation, and finally preparing and placing the base course aggregate. Preparation and construction of the subgrade and base course was monitored extensively to ensure that these materials were placed in a consistent and uniform manner.

The subgrade was built in six lifts that were approximately 15 cm deep for a total depth of about 0.9 m. The subgrade was processed to reach the target strength by adding water from a water truck and fire hose. Water was added until it reached the target moisture content (approximately 23 percent for CBR = 1.70). Processing was accomplished using a large excavator to move and mix the material as water was being added. Sufficient material was processed to construct a single 15-cm deep layer over two test sections at a time (about 30 m^3 of material). The subgrade was then placed in the trench using the excavator and a track-mounted skid-steer tractor was used to level and initially compact the subgrade. A smooth, single-drum, vibratory roller was used to compact the subgrade by making two passes of the roller in three longitudinal paths of the freshly placed subgrade. The moisture in the top surface of the subgrade was maintained during construction by periodically wetting the surface and keeping it covered with plastic until the next layer of subgrade or the base course could be placed. Prior to placement of the geosynthetics and base course, the top surface of the subgrade was smoothed and screeded to the height of the adjacent pavement surface.

Preparation of the base course aggregate began by adding water and mixing with an end loader until it reached optimum water content. A large screed that rested on the paved surface on both sides of the subgrade trench was used to level the surface of the gravel layer. The base course was placed in two layers. The final thickness of the first layer of base course was about 20 cm when compacted and the second was about 7.6 cm deep for a total of about 28 cm of gravel, on average. Two of the three control test sections contained thicker base material. The Control 2 test section was constructed of two layers of about 20 cm thick, for a total of about 40 cm of gravel when compacted, and the Control 3 test section was constructed of three layers of about 20 cm thick, and had a final average thickness of about 60 cm of gravel when compacted. Compaction was achieved using a smooth, single-drum, vibratory roller. In total, eight passes of the roller were made per lift. Assessment of the base course was evaluated using LWD, DCP, in-field CBR and nuclear densometer tests. All of the test sections met the minimum 95 percent density requirements based on Modified Proctor test results. A detailed summary and analysis of the physical attributes of the base course can be found in Cuelho et al. (2014).

4 TRAFFICKING AND DATA COLLECTION

Trafficking was accomplished using a three-axle dump truck that weighed 20.6 metric tons and had 620 kPa tire pressure. Trafficking was always in one direction, and the speed was approximately 8 kph to ensure that dynamic loads were not induced in the test sections from any

unevenness in the gravel surface. Trafficking was applied over a two-month period from mid-September to early November until rut levels reached 75 mm – defined as failure in this project. Once 75 mm of rut was reached, repairs were made by placing additional gravel in the rutted areas using a skid-steer loader to compact and level the surface. Repairs within test sections were made incrementally, so that un-failed portions of test sections could continue to be trafficked until they reached failure. No further measures of rut were made in areas that were repaired. Rut measurements were made at 1-meter intervals along two longitudinal lines, corresponding to the outside rear wheels of the test vehicle, using a robotic total station. These measurements were used to determine rut as a function of the difference in the elevation of the measurement points over time.

5 RUT ANALYSIS

Longitudinal rut measurements were the primary means used to determine the behavior and relative performance of each test section. Rut behavior is mainly affected by four factors: 1) the strength of the subgrade, 2) the depth of the base course, 3) the strength of the base course, and 4) the presence of the geosynthetic. The field test sections were constructed to have the same subgrade strength (with the intentional exception of Test Sections IFG-1 and IFG-2), the same base thickness (with the intentional exception of the Control 2 and Control 3 test sections), and the same base course strength to minimize differences between test sections and facilitate a more direct comparison between individual test sections. Despite efforts during construction to eliminate differences in subgrade strength and base course thickness, small variations were inevitable. An empirical correction procedure was implemented to adjust the rut response for these two properties so that direct performance comparisons between test sections were more accurate. Rut data was not adjusted based on base course strength and stiffness because 1) strength and stiffness properties were not measured at every rut measurement point, and 2) there were no controls where these properties were purposefully varied to determine their effect on performance. When adjustments for subgrade strength and base course thickness are applied to the rut data, the remaining behavioral differences between the reinforced test sections could more confidently be attributed to the geosynthetic reinforcement.

Individual rut measurements were adjusted and averaged together within a particular test section to create the corrected rut responses presented in Figure 2 for each of the test sections. Individual rut measurements that were greater than one standard deviation away from the mean were not used in the analysis. Test Sections IFG-1 and IFG-2 are not shown on these graphs because they were constructed for the sole purpose to formulate the corrections necessary to make direct comparisons between the remaining test sections; however, the control test sections are shown to compare performance of reinforced versus unreinforced test sections with varying depths of base course. Rut responses having steeper slopes (i.e., to the left on the graph) exhibited the poorest performance, while rut responses that were shallower (i.e., lower and to the right) showed the best performance. The woven geotextile (WoT-13) performed the best, followed by IFG-3, WeG-4 and the non-woven geotextile (NWoT-14). The poorest performance was observed in the KnG-9, WoG-7 and IFG-12 geogrids.

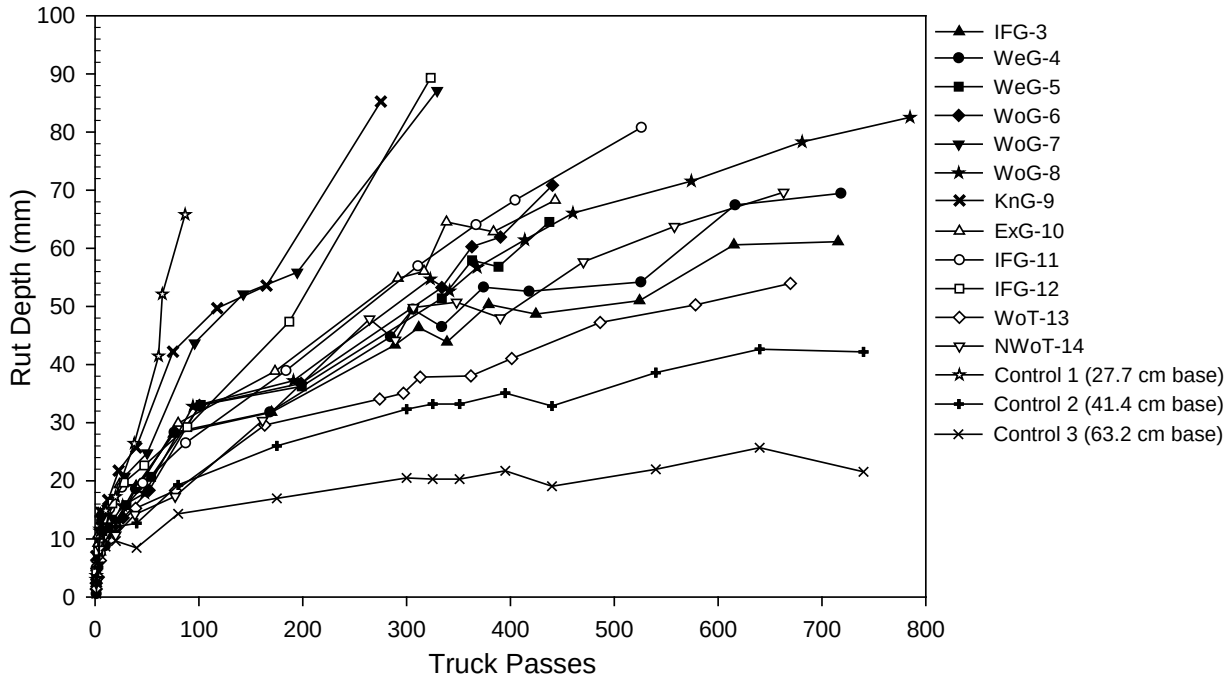

Figure 2: Corrected rut response for all test sections.

Further analysis of the longitudinal rut responses was conducted using the performance data to determine which geosynthetic material properties were most related to the performance of a particular test section. This analysis was conducted at various rut depths (25.4, 50.8 and 63.5 mm) to determine whether different material properties affected performance at various levels of rut; however, Test Sections IFG-3 and WoT-13 did not reach 63.5 mm of rut, so predicted values were used in the regression analysis at this rut level. The following material properties were considered in this analysis:

- Wide-width tensile strength at 2% (WWT-2%)
- Wide-width tensile strength at 5% (WWT-5%)
- Ultimate wide-width tensile strength (WWT-Ult.)
- Cyclic tensile stiffness at 0.5, 1.0, 1.5, 2.0, 3.0 and 4.0 percent (CTS-0.5%, CTS -1.0%, CTS -1.5%, CTS -2.0%, CTS -3.0%, CTS -4.0%)
- Resilient interface shear stiffness in the cross-machine direction (RISM)
- Junction strength in the cross-machine direction (Junc. Str.)
- Junction stiffness in the cross-machine direction, determined by taking the secant stiffness of the junction strength response at 1.3 mm of displacement (Junc. Stiff.)
- Aperture stability modulus (ASM)

Linear regression was selected because there were too few points to clearly indicate a more sophisticated regression equation and it provided sufficient information to be able to compare data fit between individual analyses or to observe changes or trends in data fit for multiple variables. In this analysis, the number of truck passes for a particular test section was adjusted by subtracting the number of truck passes in Control 1 to determine Nadd, the number of additional truck passes a particular test section experienced in comparison to Control 1. That allowed the y-intercept to be set to zero because the absence of geosynthetic reinforcement would result in no benefit to the test section. R-squared (the coefficient of determination) is commonly used as the indicator of how well the data points fit the regression line, and was used in

this analysis as the parameter to determine how well a particular material property can be used as a potential predictor of field performance. R-squared values approaching 1.0 indicate a better fit, while values less than that (including negative values) indicate poorer correlations. R-squared values greater than 0.5 were considered significant for the purposes of this analysis. The results from these analyses are shown in Figure 3a (note: the analysis of some of the properties summarized in Figure 3 and Figure 4 resulted in R-squared values less than zero, which are not shown).

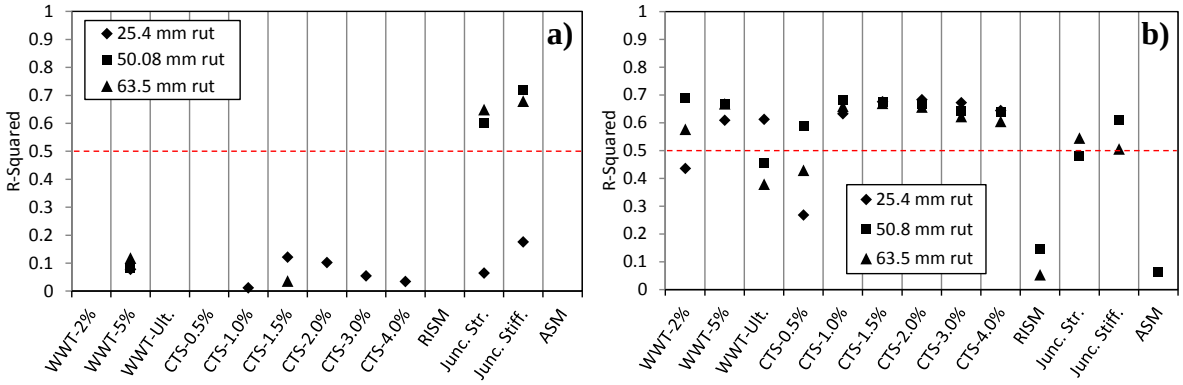

Figure 3. Regression analysis results in the cross-machine direction using a) all data and b) select data

Referring to Figure 3a, the geosynthetic material property that was most related to performance was the strength and stiffness of the junctions in the cross-machine direction, and the strength and stiffness of the junction correlated better with performance as rut increased. R-squared values in the machine direction (not shown) were all negative with the exception of the ultimate wide-width strength, which showed better correlation at lower levels of rut. A second linear regression analysis was conducted excluding data from geosynthetics that performed poorly – namely Test Section WoG-7 and Test Section KnG-9. Knowing that the primary property linked to performance in these test sections was junction stiffness, these products were unable to transmit stresses into the cross-machine structural elements because the junctions were too weak. By eliminating these products from the analysis other potential links between the geosynthetic properties and test section performance became more apparent. The results of this analysis are shown in Figure 3b. These results indicate that by excluding materials that did not perform well based on their weaker junctions, the tensile strength in the material is also a good indicator of performance. This is most apparent in the wide-width tensile strengths at 5 percent and the cyclic stiffness values. R-squared values are reduced for junction strength and stiffness because of the missing data.

A linear regression analysis was also conducted using data from Phase I of this project (Cuelho and Perkins, 2009). Six of the test sections from Phase I used the same geosynthetics as this project (IFG-3, WeG-4, WeG-5, WoG-6, WoG-8, and NWoT-14). These test sections had very similar subgrade strengths but 75 mm less base aggregate thickness, creating a more severe condition than Phase II. Performance data was analyzed with respect to the material properties listed above at 25.4, 50.8, 75 and 101.6 mm of rut. The results of this analysis are shown in Figure 4. Considering a similar approach as before, the regression analysis using performance data from the Phase I project indicates, overall, that tensile strength in both material directions relate to performance at higher levels of rut, while junction strength relates to performance at lower levels of rut. The relationship with junction strength peaks at 50.8 mm of rut, while junction stiffness peaks at 75 mm of rut. Aperture stability modulus is also related to early performance of the Phase I test sections.

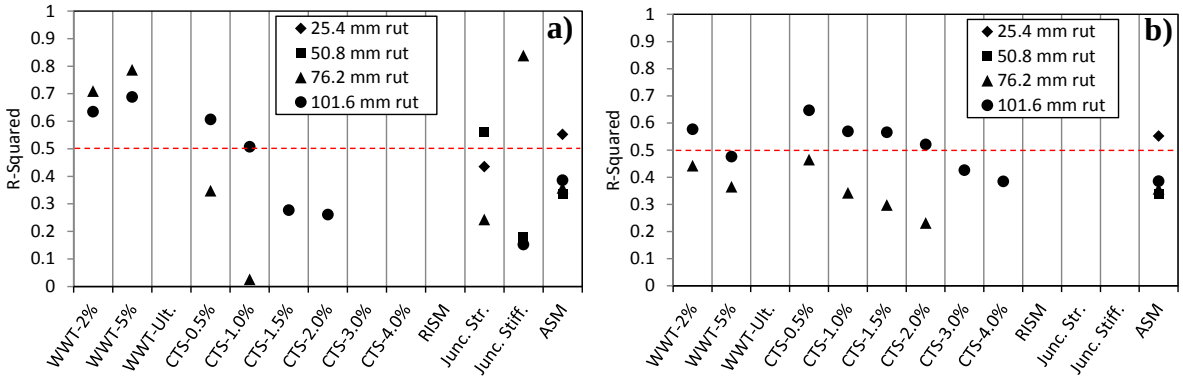

Figure 4. Phase I regression analysis results in the a) cross-machine direction and b) machine direction

Understanding that junction stiffness in the cross-machine direction is the property of the geogrids that most related to their performance it can be inferred that the mechanism by which geotextiles provide reinforcement is related to how well they transmit stresses from one principal strength direction to the other. Despite that fact that fibers oriented orthogonally to one another are not firmly bound, the interaction between them is significantly enhanced by the overburden pressure of the road materials above them. The strong frictional bond between these fibers is able to transmit stresses from traffic loads into fibers oriented in the cross-machine direction, similar to a typical geogrid junction. Multiple fibers and intersections between these fibers means that there are significantly more paths for stresses to be transmitted. This helps explain why the geotextiles worked well in this application under these conditions. A similar case can be made for the non-woven geotextile. Its tensile properties are significantly enhanced by confinement from overburden, and the continuous sheetlike structure of the material creates an infinite number of stress paths.

6 SENSOR ANALYSIS

Instrumentation was used in this research project to measure displacement and strain on the geosynthetic (in the cross-machine direction). Linearly variable displacement transducers (LVDTs) were used to directly measure displacement and resistance strain gages bonded to the surface of the geosynthetics were used to directly measure strain.

Long-term and dynamic displacement data were collected during trafficking to characterize movement and strain in the material at two locations along the west edge of the wheel path. The first displacement measurement point was furthest to the west outside of the wheel path (LVDT 1), the second measurement was near the edge of the wheel path (LVDT 2), and the third measurement point was directly under the outside tire of the dual wheel (LVDT 3), as illustrated in the plan view presented. Three separate strain calculations were also possible using these measurements. Strain1-2 is the strain between LVDT 1 and LVDT 2, Strain2-3 is the strain between LVDT 2 and LVDT 3, and Strain1-3 is the overall strain between LVDT 1 and LVDT 3. The following sign convention was used: positive displacement moves to the left (westward) in Figure 5 and positive strain indicates tension. As trafficking began, the base course aggregate began to engage the geosynthetic reinforcement as the gravel particles at the bottom of the base layer began to spread laterally under the load. The geosynthetic resisted this spreading of the aggregate by confining the particle movement primarily through interaction with the intersecting members of the grid structure or the surface friction of the textile materials. As the rut depth increased under increased truck passes, however, distortion of the rut bowl caused the gravel to gradually lose its ability to spread laterally which in turn caused the stresses in the base course layer to become more vertical, resembling punching shear.

Stresses from the loaded wheels became more vertical through the base course and the area of influence at the interface between the base and subgrade was decreased thereby increasing stresses on the top of the subgrade. As the subgrade and base were continually shoved away from the center of the rutted area under continued traffic loading, the primary mechanism of support from the geosynthetics transitioned from lateral confinement to tensioned membrane. This transition is also evident by the heaving of the subgrade and base on either side of the rut bowl (as described above) and changes in the displacement and strain characteristics.

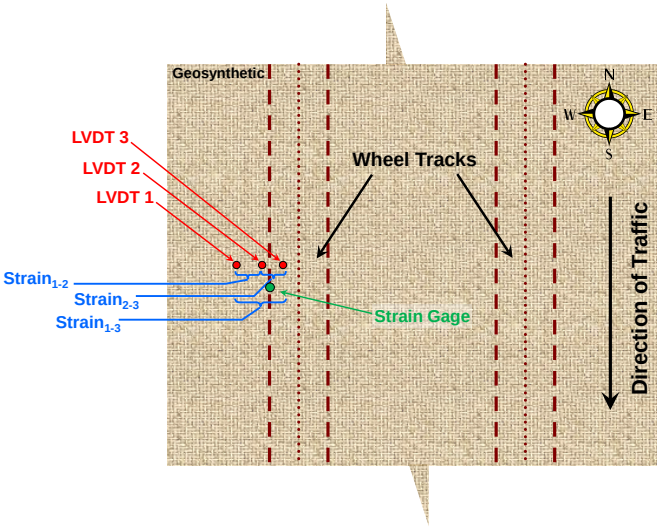

Figure 5: Illustration of displacement and strain measurements and corresponding strain calculation

Displacement of the geosynthetic as progressive rutting takes place is evident in the displacement history for each test section. Problems with the data acquisition system resulted in loss of long-term data during trafficking; however, dynamic data collected at various times during trafficking were appended together to create a continuous data trace where accumulated time between truck passes is removed to allow several truck passes to be shown on a single plot. An example history of the dynamic displacement measurements for Test Section WoG-7 is shown in Figure 6.

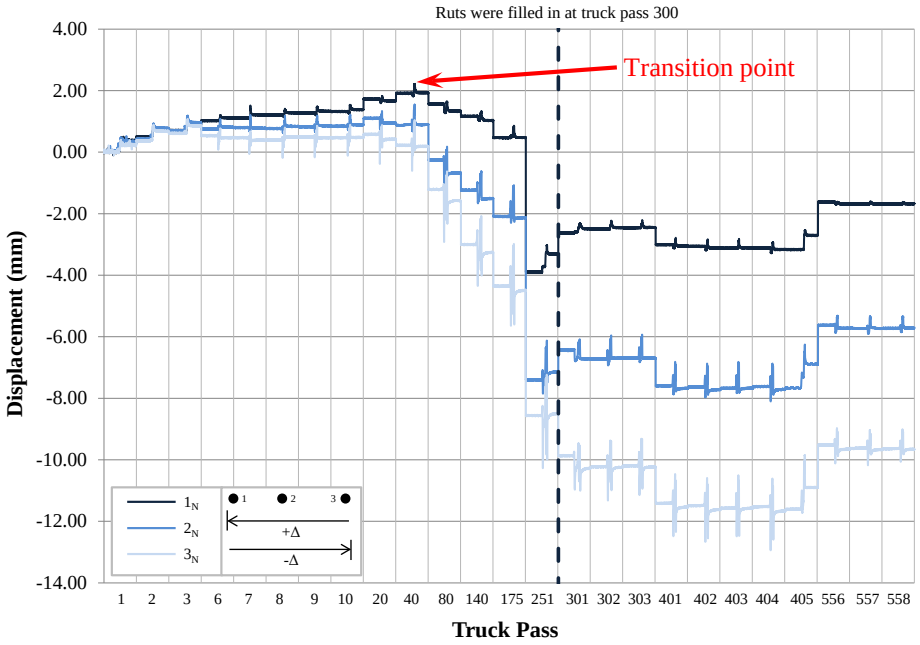

Figure 6: Example LVDT dynamic displacement results – Test Section WoG-7

Referring to Figure 6, early displacements generally accumulate in a positive direction indicating global movement of the geosynthetic to the west (away from the rutted area). After about 40 truck passes the sensors begin to move toward the rutted area as the geosynthetic is pulled down into the forming rut, as illustrated in Figure 7. This reversal of the direction in movement is coincident with the point of inflection from positive to negative slope in the displacement responses. Lateral movement of the LVDT measurement points were generally illustrated in Figure 7 using the displacement data presented in Figure 6. Similar behavior was evident in several of the test sections, with some test sections making this transition at lower or higher numbers of truck passes. This behavior suggests a transition between lateral confinement of the base course by the geosynthetic to membrane support involving deeper rutting and the tensioned-membrane effect. A graphical illustration of the point of transition for all of the test sections based on displacement data (primarily from LVDT 3 directly under the wheel at the bottom of the rut bowl) is shown in Figure 8. Changes in displacement revealed similar results to the heave (maximum height difference of rut crest and trough) and longitudinal rut response at 50.8 mm rut), namely, those test sections where the direction of the displacements transitioned earlier also reached higher levels of longitudinal rut earlier. This transition generally occurred at or before about 50.8 mm of longitudinal rut. It was not possible to determine the transition point for the IFG-11 material using the displacement data.

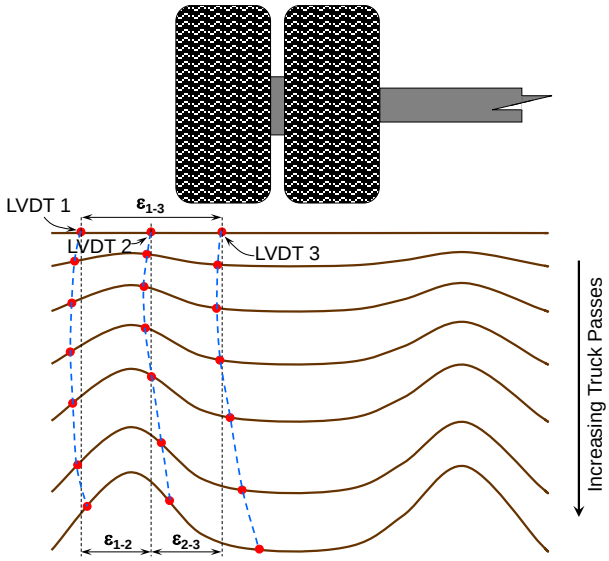

Figure 7: Distortion of the instrumented area due to rut formation.

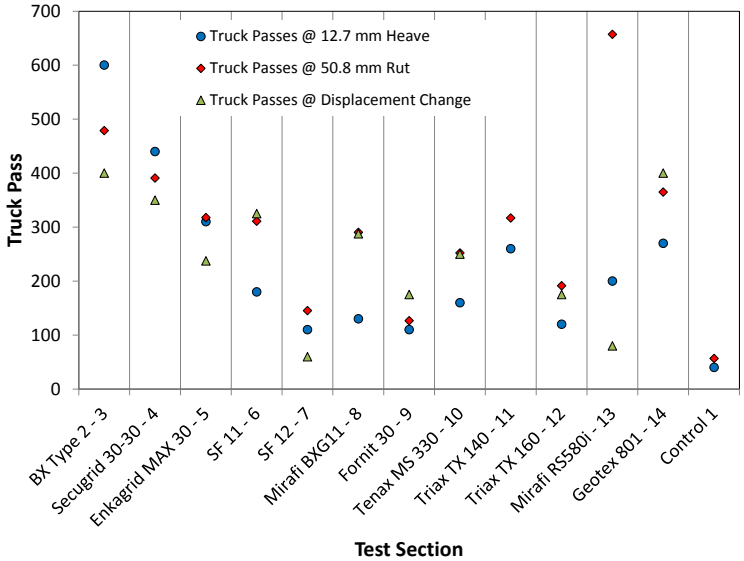

Figure 8: Heave, longitudinal rut, and change in displacement comparison for all test sections.

Similar to the displacement data, dynamic strain data (from the bonded strain gages) was used to evaluate the transition between lateral confinement of the base course by the geosynthetic to membrane support involving deeper rutting and the tensioned-membrane effect. Considering all of the test sections, maximum accumulated strains ranged from about 0.3 to 3.0 percent. The greatest strain levels were observed in NWoT-14 (non-woven textile). Considering the long-term strain data, the greatest strains in the geogrids were observed in the IFG-11 and IFG-12 test sections. The least strains were observed in the WoT-13 geotextile and WeG-4 geogrid. Working strain levels in this experiment were generally around the 2 to 5 percent range, which corresponded well with typical design properties used for these materials. Strain was also determined using the LVDTs, as discussed above and illustrated in Figure 5. Strains calculated from the displacement data varied widely, but generally were less than about 2 percent, with the exception of NWoT-14 (non-woven geotextile) which experienced strains of up to 9 percent as discerned from the long-term data.

7 SUMMARY AND CONCLUSIONS

In summary, the performance of geosynthetics as subgrade stabilization is dependent on the constructed properties of the road being stabilized. In situations where there is less structural benefit from the gravel base course layer and more benefit is expected of the geosynthetic (as in Phase I), stiffness and tensile strength play a greater role in rut suppression, especially given the rapid deterioration of these test sections under traffic load. In addition, the strength and stiffness of the junctions in the cross-machine direction plays a role, but diminishes as rut develops. Conversely, in situations where there is more base course and rut development is less rapid (as in Phase II), the role of junction stiffness and strength is more apparent as reliance on this property for performance increases as a function of rut. Coupled with this is the early dependence on the stiffness of the geosynthetic as loads are transmitted into the material, especially in the cross-machine direction as the geosynthetic confines the base aggregate as it spreads laterally under the applied load. Once the material has been engaged in this way, further transmission of lateral loads are borne by members in the machine direction of the material as they transmit the load into the cross-machine load bearing members (i.e., junction strength and stiffness).

Practitioners who wish to use these geosynthetics as subgrade stabilization should consider minimum values for geosynthetic material properties that correlated well with performance of the test sections. The material properties most related to the performance (identified as R-squared values greater than 0.5 in Figure 3 and Figure 4) included junction stiffness and strength in the cross-machine direction, wide-width tensile strength at 2 percent and 5 percent, and cyclic tension stiffness. Minimum values for these properties may be categorized by the severity of the site conditions, ranging from moderate to severe, as demonstrated in the two phases of this project. Moderate and severe conditions are subjective but can be estimated by considering the strength of the subgrade, the thickness of the base course, ground pressures associated with construction equipment, traffic levels and acceptable rut depths. Keep in mind that these properties are mutually important. For example, geogrids that have good junction strength but low tensile strength may not perform well. Likewise, geogrids with higher tensile strength and lower junction strength also may not perform well.

The woven geotextile performed well in these test sections. It can be inferred from the understanding of how geogrids transmit stresses through their junctions that the strong frictional bonds between the woven fibers (further enhanced by overburden stresses) are able to transmit stresses from traffic loads into fibers oriented in the cross-machine direction – similar to a typical geogrid junction. Multiple fibers and intersections between these fibers means that there are significantly more paths for stresses to be transmitted. Despites its relatively weak

in-air strength, the tensile properties of the non-woven geotextile are also significantly enhanced by confinement from overburden, and its continuous sheetlike structure allows for an infinite number of stress paths, allowing it to perform better than expected in this application and under these conditions.

Long-term and dynamic displacement and strain data were collected during trafficking to further characterize the transverse behavior of the test sections through the movement and strain in the material at two locations along the west edge of the wheel path. Early displacements generally accumulate in a positive direction indicating global movement of the geosynthetic to the west (away from the rutted area). After about 40 truck passes the sensors begin to move toward the rutted area as the geosynthetic is pulled down into the forming rut. This reversal of the direction in movement is coincident with the point of inflection from positive to negative slope in the displacement responses. Similar behavior was evident in several of the test sections, with some test sections making this transition at lower or higher numbers of truck passes. This behavior indicates a transition between lateral confinement of the base course by the geosynthetic to membrane support involving deeper rutting and the tensioned-membrane effect. Changes in displacement revealed similar results to the heave and longitudinal rut response, namely, those test sections where the direction of the displacements transitioned earlier also reached higher levels of longitudinal rut earlier. This transition generally occurred at or before about 50.8 mm of longitudinal rut.

8 ACKNOWLEDGEMENTS

Financial support for this pooled-fund project was generously provided by the following United States departments of transportation (listed in alphabetical order) – Idaho, Montana, New York, Ohio, Oklahoma, Oregon, South Dakota, Texas and Wyoming. Geosynthetic materials were generously donated by Colbond, Huesker, NAUE, Propex, Synteen and TenCate.

9 REFERENCES

Cuelho, E. and Perkins, S. (2009). Field Investigation of Geosynthetics Used for Subgrade Stabilization, Final report to the Montana Department of Transportation, FHWA/MT-09-003/8193, 140 pp.

Cuelho, E., Perkins, S. and Morris, Z. (2014). Relative Operational Performance of Geosynthetics Used as Subgrade Stabilization, Final report to the Montana Department of Transportation, FHWA/MT-14-002/7712-251, 328 pp.

Kinney, T. (2000) Standard Test Method for Determining the “Aperture Stability Modulus” of a Geogrid, Seattle, Shannon & Wilson, Inc.